The development of advanced vanadium alloys for fusion applications

J.M. Chen [a,c,*], T. Muroga [b], S.Y. Qiu [c], T. Nagasaka [b],
W.G. Huang [d], M.J. Tu [d], Y. Chen [c], Y. Xu [a], Z.Y. Xu [a]

[a] *Southwestern Institute of Physics, P.O. Box 432, Chengdu 610041, China*
[b] *National Institute for Fusion Science, Oroshi, Toki, Gifu 509-5292, Japan*
[c] *National Key Laboratory for Nuclear Fuel and Materials, P.O. Box 436, Chengdu 610041, China*
[d] *Sichuang University, Chengdu 610065, China*

Abstract

As an alternative choice for fusion application, V alloyed with 6–8 wt%W has been studied. The results showed that W could strengthen the alloy at room temperature, more effectively than Ti or Cr. With both additions of Ti and W, the recovery and recrystallization of the alloys behaved similarly to V–4Cr–4Ti, but the behavior was strongly influenced by the concentration of the interstitial impurities in solid solution. Similar behavior to V–4Cr–4Ti was also found for V–6W–1Ti on hydrogen embrittlement. V–6W–1Ti seemed to have better properties for hydrogen embrittlement due to its low hydrogen absorption rate. Significant differences in oxidation behavior in air were not observed for the alloys investigated.
© 2004 Elsevier B.V. All rights reserved.

1. Introduction

V–4Cr–4Ti is viewed as the leading candidate vanadium alloys as the fusion reactor structural material if a liquid lithium blanket is adopted. The alloy has the potential of high temperature application, strong resistance to neutron irradiation and feasible fabrication properties [1–3]. As an alternative choice, some V-base alloys doped with W were studied recently [4]. The addition of W was expected to further increase the high temperature strength and creep properties of the alloy. So far, basic studies on the recovery and recrystallization behavior, hydrogen embrittlement, and the strengthening of W have been conducted. This paper reports the highlight of these studies.

2. Experimental procedure

2.1. Alloy preparation

Alloying V with Cr, Ti, W, Al has been evaluated. The alloy compositions were V–4Cr–4Ti, V–6W–(1–4) Ti, V–8W, V–7W–0.3Al and V–4Ti. Small ingots of ∼350 g each were prepared from the mechanical mixture of pure metals by induction melting in a magnetic floating furnace. The ingots were then forged, hot-rolled and cold-rolled to 0.25–1 mm thick plates for the experimental testing. The details of alloy preparation have been reported elsewhere [4]. Table 1 lists the results of the chemical analysis, which was performed on the cold-rolled plates.

2.2. Hydrogen charging and tensile tests

Tensile specimens were cut from the 980 °C annealed plates with gauge dimensions of $25 \times 8 \times 0.5$ mm^3. The specimens, together with ZrH$_{1.8}$ hydride in a weight ratio of 0.1 above the specimen weight, were enclosed in

Table 1
Chemical compositions of the V-base alloys and the vacuum annealing temperature (T) prior to cold rolling

Alloy	Chemical composition (wt%), C, N, O (wppm)								T (°C)
	W	Si	Ti	C	N	O	Cr	Al	
V–8W	8.28	0.014	–	100	40	230	–	–	980
V–7W–0.3Al	7.35	0.014	–	110	30	290	–	0.34	980
V–6W–1Ti–N	6.48	0.014	1.10	90	30	250	–	0.12	980
V–4Ti	<0.5	0.014	3.99	120	30	280	–	–	980
V–6W–1Ti	6.04	<0.01	1.07	70	5	350	<0.05	<0.01	850
V–6W–2.5Ti	5.56	<0.01	2.53	80	5	370	<0.05	<0.01	850
V–6W–4Ti	5.64	<0.01	4.12	50	4	350	<0.05	<0.01	850
V–4Cr–4Ti	<0.5	0.01	4.19	60	3	350	4.18	<0.01	850

evacuated quartz tubes for hydrogen charging. Each tube had a diameter of ∼20 mm and a length of ∼200 mm, and a vacuum in the level of 10^{-5} Torr. The tubes were heated to 800 °C and kept at the temperature for different time up to 3 h, then water quenched to room temperature.

Hydrogen concentration in the specimens was measured with a RH404 type hydrogen-measuring device that was made by the Leco Co. in the United States. Tensile tests were performed on an Instron 4302 machine at room temperature in air, with the strain rate of $1.1 \times 10^{-3} \text{s}^{-1}$. The total and uniform elongations were determined from the engineering stress-strain curves.

2.3. Hardness recovery test

Samples for the recovery and recrystallization experiments were cut from the ∼50% cold-rolled plates in a size of 10×5 mm². Vacuum annealing was conducted at 850 or 980 °C for 1 h prior to the cold rolling. The temperature (T) was also shown in Table 1. After mechanically grinding and electro-polishing, the samples were annealed at temperature of 100–1100 °C for 1 h in a vacuum less than 1×10^{-6} Torr. The microstructures of the samples were analyzed using scanning electron microscope (SEM) and transmission electron microscope (TEM). Vickers hardness tests with a load of 500 g and a duration of 30 s were conducted after the annealing.

2.4. Oxidation in air

Oxidation was performed in air at 400, 500 and 600 °C up to ∼200 h. The samples had dimensions of $10 \times 10 \times 1$ mm³. Weight gain was measured and X-ray diffraction (XRD) was used to identify the surface oxidation products.

3. The mechanical strength of the alloys

Fig. 1 shows the tensile properties for some of the alloys. In the figure the strengthening by W is shown.

Both the yield strength and the ultimate tensile strength increased with increasing W concentration, while the tensile elongations did not change much with the exception of V–7W–0.3Al. This alloy has relatively higher uniform elongation and much higher total elongation than the others, which was thought to be the result of the Al addition. Al could generally result in high ductility due to the reduction of the oxygen concentration in the V-base alloys [5].

The hardness was measured for some of the alloys at room temperature to assess the solid solution hardening of the alloying elements. The samples were annealed at 1100 °C for 1 h to obtain a full solid solution state. Fig. 2 shows the dependence of the Vicker's hardness on the Ti concentration in the V–6W–Ti alloys. The hardness increased with Ti. The increasing rate was about 8.87 H_v/%Ti based on a linear correlation. In order to get the hardening coefficient more precisely, the contribution of other impurities in the alloys must be removed. Eq. (1) gives a relation among the hardness (H_v) and the con-
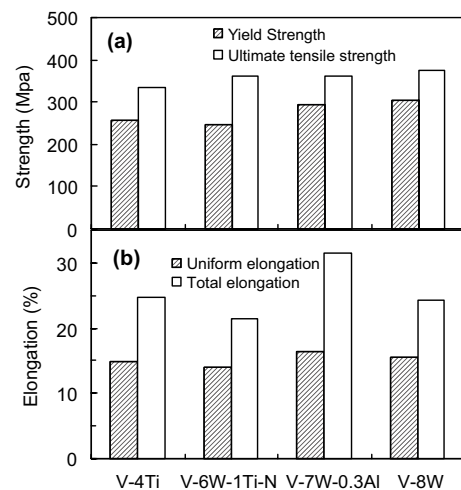

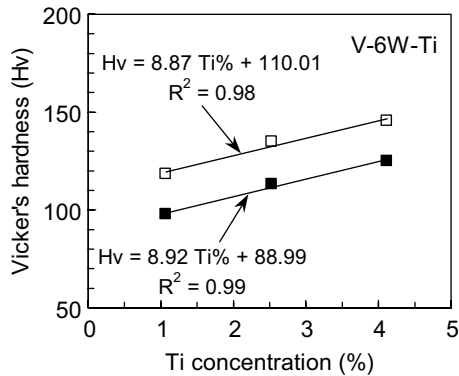Fig. 1. The tensile properties of the alloys at room temperature.

Fig. 2. The hardness of the V–6W–Ti alloys in solution-annealing state. Solid symbol: contribution of the O and N were subtracted.

Fig. 3. The dependence of the hardness on the annealing temperature, showing the influence of the nitrogen concentration in V–6W–1Ti.

centrations of the species (C_m) in an alloy based on solid solution hardening assumption.

$$H_v = H_0 + \sum_m H_m C_m. \tag{1}$$

Here H_m is the hardening coefficient of the solid solution species and H_0 is a constant. From the previous studies by Nagasaka, et al. [6], the hardening coefficient of N, O and H_0 in unalloyed V was about 0.12, 0.057 and 48, respectively. Assuming that the coefficients are not changed in the present alloys, the contribution of the impurities to the hardness was subtracted. The solid square symbols in Fig. 2 show the results. The hardening coefficient of Ti, thus, is about 8.92 Hv/%mass. The remaining contribution of ~6%W and H_0 is about 88.99 H_v. Therefore, the hardening coefficient of W in the alloys is about 7.13 H_v/%mass, which is a little lower than that of Ti. The hardness of the V–4Cr–4Ti alloy was measured to be 145.6 H_v. In the same way, the hardening coefficient of Cr in V–4Cr–4Ti alloy was calculated to be about 9.55 H_v/%mass. So Cr contributed more strongly to the solid solution hardening than Ti. Considering the much bigger atom weight of W, W should be the strongest species per atom to strengthen the alloy at room temperature.

4. Recovery and recrystallization

Some of the results have been reported in Ref. [4]. The results showed that both V–8W and V–7W–0.3Al behaved similarly to unalloyed V, while V–4Ti behaved like the NIFS-Heat2 (V–4Cr–4Ti) alloy. Hardness of V–4Ti began to recover at 600 °C, which was higher than V–8W and V–7W–0.3Al due to the precipitation in V–4Ti. It was also reported that the temperature required for the hardness recovery for V–6W–1Ti–N (with 30
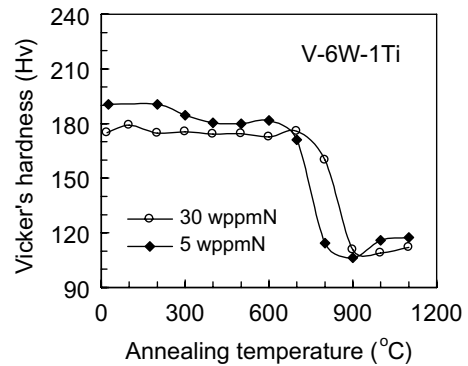
wppm N) was ~700 °C where additional hardening occurred. The hardening was thought to be the result of interactions between the dislocations and the interstitial impurities. However, this was not the case for V–6W–1Ti with 5 wppm N (Fig. 3). It seems that N has played a more important role in the interactions than the other interstitial impurities such as O.

SEM observation of the etched samples indicated that recrystallization was nearly completed for all of the alloys at 900 °C. TEM observation showed that the number of large precipitates in the alloys decreased with increasing temperature above 900 °C. The number was thought to be higher in V–6W–1Ti than that in V–6W–1Ti–N before the last annealing, because the former alloy had ever taken the annealing at 850 °C but the latter one at higher temperature of 980 °C prior to the cold rolling (see Table 1). The precipitate contains Ti, C and probably N and O. Precipitation decreases the concentration of the interstitial impurities in solid solution. As a result, the mobile interstitial impurities in V–6W–1Ti were thought to be fewer than those in V–6W–1Ti–N. Consequently, the interactions between the interstitial impurities and the dislocations were weaker in V–6W–1Ti during the last annealing, leading to the more pronounced hardness recovery of V–6W–1Ti compared with V–6W–1Ti–N at 700 °C and above.

Nagasaka et al. reported that the additional hardening at ~300 °C was strongly dependent on the nitrogen concentration in unalloyed V, while the effect of O was much weaker [6]. Strengthening by DSA (dynamic strain aging) was also found in V–4Cr–4Ti alloy during high temperature tensile tests [7]. N was thought to be the main contributor to the DSA at high temperature [2]. Thus the disappearance of the hardening at 700 °C for V–6W–1Ti is partially ascribed to its quite low nitrogen concentration.

5. Hydrogen effects

Fig. 4(a) shows the accumulation of the hydrogen in the alloys as a function of the exposure time. The figure suggests that the hydrogen concentration approached saturation with increasing exposure time, and clearly shows that the addition of Ti or Al to V promoted the hydrogen absorption, while the effect of W was much weaker. The enhancement was thought to be due to the strong affinity and solubility of Ti for H. It has been found that the hydrogen solubility in V–Ti binary alloys increases with titanium content [8].

Fig. 4(b) shows the ductility of the alloys as a function of the hydrogen concentration. The figure shows superior hydrogen embrittlement resistance for the Ti-bearing alloys. Alloying V with Ti seems to be an essential requirement for better properties related to hydrogen embrittlement.

It was well known that Ti is a strong scavenging species for interstitial impurities, thus, may bind hydrogen, resulting in a decreased interaction between the hydrogen and the dislocations in the alloy. It was reported that Ti could decrease the diffusion coefficient of hydrogen in the Ti-bearing alloy [9].Consequently the effect of the hydrogen on the tensile properties is thought to be smaller. Natesan et al. [10] reported that the critical hydrogen concentration required to embrittle the
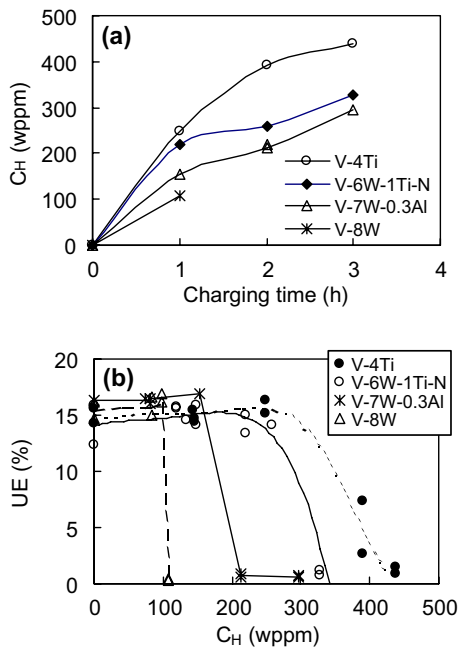
US V–4Cr–4Ti alloy (Heat #832665) is about 360 wppm based on their tensile test results. A previous study showed this concentration was in the range of 215–310 wppm H for the NIFS-Heat2 V–4Cr–4Ti alloy with an increase in oxygen concentration to 300–400 wppm, caused by high temperature hydrogen charging [11]. From Fig. 4(b), the critical hydrogen concentration for the V–6W–1Ti alloy is at a similar level to that of the NIFS heat.

6. Oxidation in air

Oxidation kinetics of the alloys at temperature from 400 to 600 °C is shown in Fig. 5(a). All of them exhibited parabolic behavior, indicative of diffusion controlled oxidation processes. The correlation between the weight gain (ΔW) and the exposure time (t) could be expressed as $(\Delta W)^2 = K_p \cdot t$, where K_p is a parabolic rate constant. It was found from Fig. 5(b) that the parabolic rate constant is independent of the alloy composition and increases with increasing temperature.

The slope of the curves in Fig. 5(b) could give a rough estimation of the activation energy of the oxidation process. The figure shows that the activation energy decreases with increasing temperature. It is supposed that oxygen could diffuse through the oxidized layer much easier at higher temperature. With

Fig. 4. The hydrogen absorption behavior (a) and the dependence of the uniform elongation (UE) on the hydrogen content (C_H) (b).
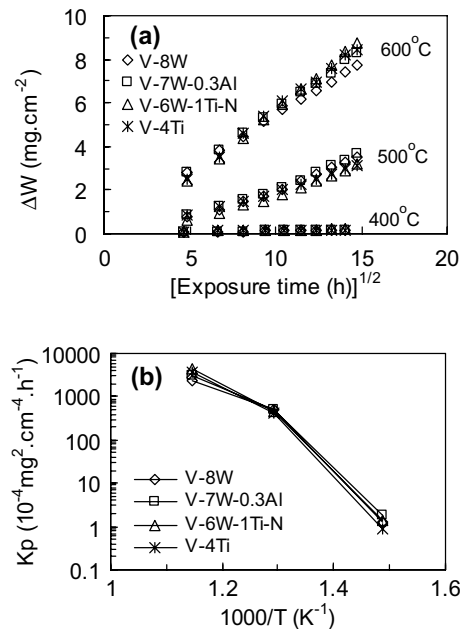

Fig. 5. Weight gain plotted against the square root of exposure time (a) and parabolic rate constant as a function of the reciprocal of the temperature (b).

XRD analysis, it was found that the dominant oxidizing products were VO_2 at temperature of 500 °C and below, but V_2O_5 at 600 °C. V_2O_5 is volatile and unstable at the temperature, is thus considered to be a weak protection layer.

7. Conclusions

Some V-base alloys with W addition were produced. Their recovery and recrystallization behavior, strengthening by alloying, hydrogen embrittlement, and oxidation in air have been investigated. The results are summarized as follows:

(1) Tungsten can strengthen the alloy greatly at room temperature, more effectively than Ti or Cr.
(2) The concentration of interstitial impurities in solid solution has strong effect on the hardness recovery of V–6W–1Ti.
(3) The addition of W did not influence the hydrogen embrittlement properties. Ti is an essential element to maintain high resistance to hydrogen embrittlement, although it enhances the hydrogen absorption.
(4) The oxidation of the V–W–Ti alloy in air obeys a parabolic kinetics with small effects of the alloying elements.

References

[1] T. Muroga, T. Nagasaka, K. Abe, V.M. Chernov, H. Matsui, et al., J. Nucl. Mater. 307–311 (2002) 547.
[2] K. Fukumoto, T. Yamamoto, N. Nakao, S. Takahashi, H. Matsui, J. Nucl. Mater. 307–311 (2002) 610.
[3] T. Nagasaka, N.J. Heo, T. Muroga, M. Imamura, Fusion. Eng. Des. 61&62 (2002) 757.
[4] J. Chen, T. Muroga, T. Nagasaka, Y. Xu, S. Qiu, J. Nucl. Mater. 322 (2003) 73.
[5] J. Chen, S. Qiu, L. Yang, Z. Xu, Y. Deng, Y. Xu, J. Nucl. Mater. 302 (2002) 135.
[6] T. Nagasaka, H. Takahashi, T. Muroga, T. Tanabe, H. Matsui, J. Nucl. Mater. 283–287 (2000) 816.
[7] D.T. Hoelzer, A.F. Rowcliffe, J. Nucl. Mater. 307–311 (2002) 596.
[8] H. Bleichert, H. Wenzl, Phys. Stat. Sol. B 144 (1987) 361.
[9] S. Yano, M. Tada, H. Matsui, J. Nucl. Mater. 179–181 (1991) 779.
[10] K. Natesan, W.K. Soppet, J. Nucl. Mater. 283–287 (2000) 1316.
[11] J. Chen, T. Muroga, S. Qiu, Y. Xu, Y. Den, Z. Xu, J. Nucl. Mater. 325 (2004) 79.